A stochastic MIMO model for far-end crosstalk in VDSL cable binders

Conference Paper · July 2009

DOI: 10.1109/ICC.2009.5198675 · Source: IEEE Xplore

3 authors, including:

Wen Xu
Institute of Electrical and Electronics Engineers

W. Xu, C. Schroeder, P. A. Hoeher, “A Stochastic MIMO Model for Far-End Crosstalk in VDSL Cable Binders” in *Proc. International Conference on Communications (ICC)*, Dresden, Germany, June 2009.

This full text paper was peer reviewed at the direction of IEEE Communications Society subject matter experts for publication in the IEEE ICC 2009 proceedings

A Stochastic MIMO Model for Far-End Crosstalk in VDSL Cable Binders

Wen Xu
Infineon Technologies AG
Am Campeon 1-12, 85579 Neubiberg, Germany
Email: wen.xu@ieee.org

Christian Schroeder and Peter Adam Hoeher
Information and Coding Theory Lab, University of Kiel
Kaiserstr. 2, 24143 Kiel, Germany
Email: {csc,ph}@tf.uni-kiel.de

***Abstract*—Future digital subscriber line (DSL) systems are supposed to achieve higher data rates by using interference cancellation techniques. Since far-end crosstalk (FEXT) is the major impairment in DSL systems based on frequency division duplexing, mitigation of this interference can increase the signal-to-interference-and-noise ratio, and therefore significantly boost the data rate. For simulation and evaluation of FEXT cancellation algorithms, more accurate modelling of the multiple-input-multiple-output (MIMO) crosstalk channels is needed. Until now, DSL standards usually rely on the 99% worst case modelling of crosstalk power-sum for the lines in a binder. This paper proposes a parametric stochastic FEXT model based on the sum-of-sinusoids approach for the pair-to-pair crosstalk among multiple lines in a binder, which shows a more realistic behaviour than the worst case models.**

***Index Terms*—DSL, dynamic spectrum management, crosstalk, FEXT cancellation, MIMO channel modelling**

I. Introduction

For digital subscriber line (DSL) systems such as ADSL and VDSL, dynamic spectrum management (DSM) has been proposed to increase data rate by adapting the transmit PSD (power spectral density) to the crosstalk noise on the line (see e.g. [1]). Especially DSM level 3, also known as DSL MIMO or vectoring, is supposed to achieve significant gains by using joint signal processing for lines in a binder at the central office (CO). It aims at reducing the crosstalk interference between the lines in a binder, especially the far-end crosstalk (FEXT) which is the major impairment in ADSL and VDSL systems. Some examples for measured FEXT transfer functions are depicted in Fig. 1.

To evaluate FEXT cancellation algorithms and to estimate the achievable gains, a more realistic channel model describing the coupling coefficients among transmitting (disturbing) lines and receiving (victim) lines is desired, especially when no real FEXT measurement data are available. Until now, worst case models for the near-end crosstalk (NEXT) and the FEXT are commonly used [2]. For a cable line, so-called 99% worst case NEXT and FEXT models, as described in the DSL standards [3], provide an estimate of the crosstalk power from the other lines in a binder. In 99% of the cases the crosstalk power is less than that predicted by the model. Specifically, the FEXT power transfer function according to the 99% worst case model is given by

$$|H_{Fext,WC}\,(f,n,l_c)\,|^2 = n^{0.6} f^2 l_c X_F |H_L\,(f,l)\,|^2 \qquad (1)$$

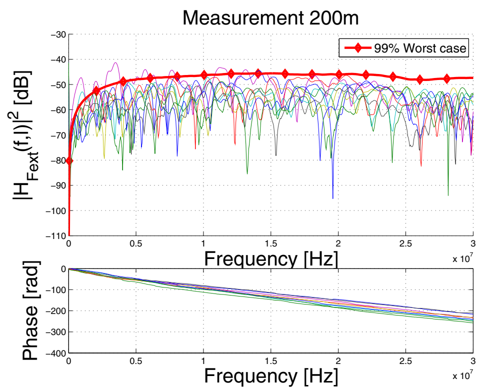

Fig. 1. Example of measured FEXT transfer functions of 200m cable (magnitude and phase).

where n is the number of active lines in the binder, f is the radio frequency (which can be up to 30 MHz for the current VDSL), l is the line length from the transmitter to the receiver, l_c is the coupling length of the lines (distance between disturbing transmitter and victim receiver), $X_F = 7.74 \cdot 10^{-21}$ (for l_c given in ft) is an empirical worst case constant for an American 50-pair AWG22 cable, and $H_L(f,l)$ is the line transfer function between disturbing transmitter and victim receiver. In the following, we may omit the explicit dependency of the FEXT on the parameters n as well as l_c and simply use $H_{Fext,WC}\,(f)$ for conciseness.

Notice that these worst case estimations neither consider irregular variations with frequency for a single pair-to-pair coupling (as visible in Fig. 1) nor the phase coupling between two lines, so that they are not suitable, say, for evaluating crosstalk cancellation algorithms. Therefore, attempts have been made to overcome these constraints and to more accurately model the crosstalk.

The remainder of the paper is organized as follows: Section II gives an overview on recently reported crosstalk models for the FEXT. In Section III, a new modelling approach using the sum-of-sinusoids approach is presented. Section IV analyzes the statistical properties of the presented model against the measurement data. In Section V, some concluding remarks are given.

978-1-4244-3435-0/09/$25.00 ©2009 IEEE

II. Overview on Available Channel Models

Besides the worst case models, several models have recently been proposed for crosstalk modelling. These models can be divided into two classes: 1) *stochastic models* which extend the worst case models with random variables for amplitude and phase variations and, 2) *physical models* using cascaded small segments to calculate the interference caused by other lines in a binder.

A. Stochastic Models

With the stochastic models, phase coupling is usually modelled as uniformly distributed since measurements show a nearly linear phase behavior over frequency (cf. Fig 1). In general, these models can be expressed as

$$H_{Fext}\left(f\right) = H_{Fext,WC}\left(f\right) 10^{\frac{X_{dB}(f)}{20}} e^{j\varphi(f)} \tag{2}$$

where $X_{dB}(f)$ is a random offset given in decibel, modelling the amplitude variations over frequency, and $\varphi(f)$ is a uniformly distributed phase. The distribution of $X_{dB}(f)$ can be determined from measurements and is usually assumed to be Gaussian [4] or Beta distributed [5]. Though the amplitude variations in measured FEXT strongly depend on frequency, $X_{dB}(f)$ is approximately treated as a constant X_{dB} for all frequencies (see e.g. [4], [6]).

Similarly, $\varphi(f)$ is usually modelled to have the same slope as the direct line phase with a statistical offset [7]. The shape parameters A and B of the Beta distribution are empirically found to be $A = 11$ and $B = 6.6$ with an extended range of values from -60 dB to 10 dB. For better resemblance of the geometric cable structure consisting of several binders, X_{dB} is also varied with an additional offset value depending on the location of the lines in the binders. With this simplification a sample pair-to-pair coupling function constructed by the model results in a shifted replica of the worst case curve, shifted by a value drawn from the random offset variable X_{dB}. So for a number of FEXT couplings the models generate several curves, each with a random but constant offset. The frequent and irregular FEXT variations with frequency have not been taken into account in these models. A model proposal going in a similar direction is given in [8] and in an earlier version in [9]. Here, the frequency variations are approximated by cosine functions. The model in [8] uses an additional cosine term with random parameters instead of a constant offset variable X_{dB}

$$\begin{aligned} H_{Fext}\left(f\right) = {} & \sqrt{l_c X_F}(n-1)^{-0,2} f |H_L(f,l)| \\ & \cdot e^{j(2\pi f\tau+\varphi)} \cdot \left[1 + \alpha\cos\left(2\pi f\beta + \gamma\right)\right] \end{aligned} \tag{3}$$

with random variables α, β, γ and φ which have to be chosen to fit measurement data and a parameter τ to get a causal impulse response. By comparing this model with (1), we see that the worst case formula is also included here, and is extended by incorporating a cosine term which very roughly approximates the FEXT variation with the frequency. However, the single cosine term leads to a strongly deterministic and regular behaviour with equidistant notches for a given set of random values.

B. Physical Models Based on Cascaded Segment

In contrast to pure stochastic models, models based on cascaded segments have a solid physical background. The basic idea is that the cable binder can be considered as cascade of many small and homogeneous segments. For each segment the transfer function matrix is determined by the cable parameters. Building the segments usually involves the use of the primary transmission line parameters. Hence, these models involve a smaller degree of abstraction and are based more on the physical reality than the stochastic ones.

The most detailed model is given by Lee [10]. Here, for each cable segment i consisting of N twisted wire pairs (TWP), matrices for the primary transmission line parameters are calculated which leads to chain matrices with a size of $[4N-2] \times [4N-2]$. These chain matrices are then cascaded to build an overall chain matrix for the whole cable. The main drawback of such segment-based models is the high computational complexity due to the extensive use of matrix operations and inversions. Especially for a large number of lines N, the complexity may be so high that employing the model in practice becomes very difficult.

III. Stochastic Modelling Based on Sum-of-Sinusoids

In this section, we describe a new stochastic model. It has much less computational complexity than the physical model based on cascading small cable segments, but can well resemble realistic measurement data. We start with the simple model given in (3). To overcome the constraints of this model, the cosine term is first extended to a sum of K_0 sinusoid terms, each having a set of random variables α'_k, β'_k and γ'_k, for $k = 1 \ldots K_0$. The scaling factor $(n-1)^{-0,2}$ in (3) is omitted. As such, the following model can be obtained:

$$\begin{aligned} H_{Fext}(f) = {} & H_{Fext,WC}(f) e^{j(2\pi f\tau+\varphi)} \\ & \cdot \sum_{k=1}^{K_0} \alpha'_k \cos\left(\beta'_k f + \gamma'_k\right) \end{aligned} \tag{4}$$

The sum-of-sinusoids channel modelling approach has extensively been applied to the simulation of *wireless* fading channels (see e.g. [11], [12], [13]). It is, to the authors' knowledge, not yet been employed to the simulation of *wireline* channels. Such a model can in general also be expressed using complex exponentials instead of the cosine terms. Similar to the existing stochastic models, the phase is derived from the direct channel's phase and modelled separately. Then, the magnitude of the model can be written as

$$|H_{Fext}(f)| = H_{Fext,WC}(f) \left| \sum_{k=1}^{K} \alpha_k e^{j(\beta_k f + \gamma_k)} \right| \tag{5}$$

With the separately modelled phase, (5) is equivalent to (4). In fact, for the magnitude it can easily be shown that $K_0 = \frac{K^2-K}{2}$ holds. Other parameters α_k, β_k, etc. can be derived accordingly (see [14] for details).

A. Modelling the Magnitude

To model the magnitude of the FEXT, the random variables have to be characterized accurately. This is done by a nonlinear least-squares curve-fitting of measured FEXT magnitudes. The used fitting function is a sum of $K = 8$ sinusoids[1] having three parameters each, expressed by

$$H_{fit} = \sum_{k=1}^{K} a_k \sin\left(b_k f + c_k\right) \tag{6}$$

The parameters are chosen in the least-squares sense to minimize the quadratic fitting error.

For this paper, the following two sets of measurement data were used:

1) 150m, 300m and 600m cable length, wire diameter 0.35mm
2) 100m, 200m and 400m cable length, wire diameter 0.4mm

Cables from both sets had 50 pairs per cable and 5 starquads per binder. The FEXT was measured inside one binder and to an adjacent one. With these data sets, 90 intra-binder FEXT transfer functions were available for the analysis. For the fitting, the measured complex transfer functions were normalized w.r.t. the worst case model given in (1). The main advantage becomes aware when the curves are synthesized from the fitting parameters since conformity with the worst case is guaranteed when the curves are multiplied by the worst case again. The fitting itself was done separately for real and imaginary part of the normalized FEXT.

Further analysis is based on data from fitting to the real part. The model parameters α_k, β_k and γ_k are now derived from the fitting parameters a_k, b_k and c_k. After fitting with $K = 8$ sine terms, 24 parameters per fitted measurement curve were obtained. For simplicity, the analysis was focussed on a_k and b_k only, whereas for γ_k a uniform distribution was assumed. The fitting parameter pair a_k and b_k for one curve defines the used sinusoids in amplitude and frequency, respectively. The idea was to find a relation between the a_k and b_k for all measurements. For this purpose the tuples $[a_k, b_k]$ for each curve were sorted to ascending b_k values. For different k the values of b_k are very similar whereas the corresponding a_k show a larger spread. At each index k, the median $\tilde{\mu}_k$ and the standard deviation σ_k of the sorted curves (in logarithmic scale) are calculated. As obvious from the figure, the standard deviation is small for the frequency parameter b_k, but has to deal with larger spread values for the amplitude parameter a_k. With the median and the corresponding standard deviation, a Gaussian distribution of the values at each index is assumed. Then, the model parameters α_k and β_k can be obtained by random draws from that distribution at the corresponding index. The fitting parameters a_k and b_k from the 90 measured curves per cable length reduce to only two curves (median and standard deviation over index number) for each set of the

[1] The value of K was constrained here due to the capability of the implemented software as well as the computer used. In general, the higher K is, the more accurate the fitting will be.

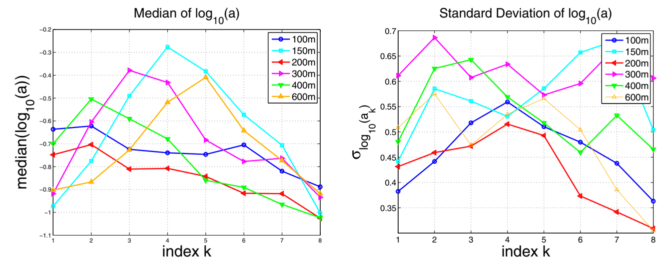

(a) Median (b) Standard deviation

Fig. 2. Medians and standard deviations of parameter $\log_{10} a$ at fitting indices k for different cable lengths.

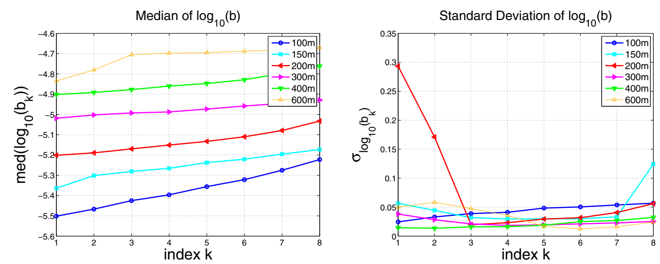

(a) Median (b) Standard deviation

Fig. 3. Medians and standard deviations of parameter $\log_{10} b$ at fitting indices k for different cable lengths.

parameters and a specific length. For generation of modelled FEXT transfer functions, for each index k a random draw from a Gaussian distribution with the corresponding parameters at that index is performed. In the synthesis, also $K = 8$ is chosen. To use a higher number of sinusoids for generating the curves, the median and standard deviation curves need to be interpolated. For the used lengths, the obtained median and standard deviation curves are depicted in Figs. 2 and 3. A first look at the frequency parameter $\log_{10} b$ (see Fig. 3 (a)) shows that the median curves for the indices $k = 1 \ldots K$ are almost parallel and the standard deviations have almost the same values for almost all cable lengths. This gives a good reason for a length-independent approach with universal parameters which can also model loop lengths not supported by measurements. The amplitude parameter $\log_{10} a$ instead does not show such a homogeneous behavior for the different lengths. But the median curves in Fig. 2 (a) allow to distinguish between the two measurement data sets. For measurements from the data set #1 the curves have a maximum around the indices $k = 3 \ldots 5$ whereas the curves from the data set #2 have a flatter shape but look similar to each others. For the standard deviations of $\log_{10} a$, the curves from the different lengths seem to follow no visible rule.

For synthesis of FEXT magnitudes these properties of the statistical parameters allow a rough approximation for an all-length modelling approach with Gaussian distributed parameters having parameters $(\mu_\alpha, \sigma_\alpha)$ and $(\mu_\beta, \sigma_\beta)$. The standard deviations σ in logarithmic scale are set to fixed values for all lengths: $\sigma_{\log_{10}\alpha} = 0.55$ and $\sigma_{\log_{10}\beta} = 0.02$ for simplicity. The median value of b_k is approximated in logarithmic scale referenced to the 100m curve in Fig. 3 (a) with $\nu = \frac{l}{100m}$ by the length-dependent relation

$$\tilde{\mu}_{\log_{10} b_k,\nu} = -5.5 + \delta(\nu) \cdot k + \log_{10}(\nu) \tag{7}$$

with a length-dependent slope

$$\delta(\nu) = 0.3/8 \cdot 1/\nu \tag{8}$$

for the mean value $\mu_{\log_{10}\beta}$ of a Gaussian distribution. The values for $\mu_{\log_{10}\alpha}$ are taken from the median of the 300m curves which produced good results.

Furthermore, our simulation results reveal that the mean values of model and measurement differ by roughly 5 dB. To compensate for this, the resulting FEXT magnitudes were properly scaled to fit the available measurement data. This scaling factor was obtained from comparing the mean values of the measured FEXT magnitudes and those of the model output.

B. Modelling the Phase Coupling

The phase coupling $\varphi_{Fext}(f, l)$ is modelled separately from the magnitude. As could be seen from the measurements, the FEXT phase is approximately linear like the phase of the direct channel $\varphi_L(f, l)$, but with different slope. Some contributions (e.g. [15]) propose to simply use the phase of the direct channel as supported by the underlying measurements. In the measurements available for this paper, the phases of the FEXT and the direct channel were not identical. Therefore, the phase modelling is achieved by varying the slope of the direct channel phase (which is linear) by a random variable according to the measured distribution of the phase slope. This approximation neglects the effect of the phase not being a straight line but changing the slope slightly.

The measured FEXT phase curves all lie below the direct channel phase. According to the spread in the phase slope a random variable φ_0 is introduced to randomize the direct channel slope. Hence, the phase is modelled by

$$\varphi_{Fext}(f, l) = \varphi_L(f, l) \cdot \varphi_0 \tag{9}$$

with φ_0 being Gaussian distributed with mean $\mu_{\varphi_0} \approx 1.3$ and $\sigma_{\varphi_0} \approx 0.09$. These values are roughly chosen for the slope variations since they do not include the influence of the length. In fact, the phase slope can vary for different cable lengths. Realizations of the implementation of this modelling approach are given in Fig. 4.

IV. Statistical Analysis

In this section, we compare the statistical properties of the model output data and the underlying measurement data. Ideally, the statistical parameters of both the measurement and model data should be nearly the same in order to justify the reasonability and usefulness of the presented model.

A. Statistics of Measurement Data

Here, the statistical properties of the measurement data serve as the reference for the model data.

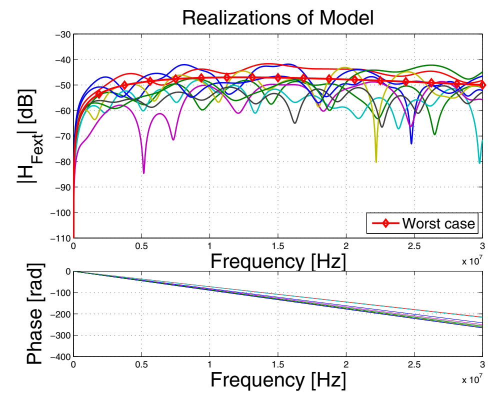

Fig. 4. Realization of the proposed FEXT model for 200m cable.

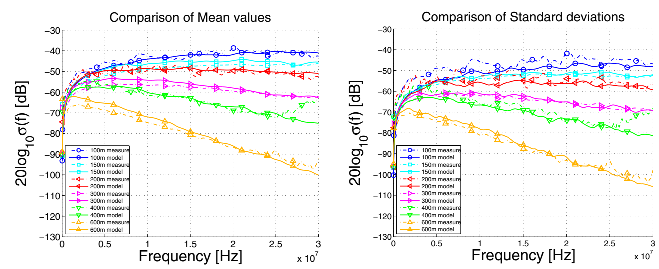

(a) Mean (b) Standard deviation

Fig. 5. Mean values and standard deviations of measured and modelled FEXT magnitudes.

1) First order statistics: Beginning with the first order statistics, Fig. 5 (a) shows the mean value of the power transfer function $|H_{Fext}(f)|^2$ for the available cable lengths in the dash-dotted curves. Fig. 5 (b) shows the standard deviations of the magnitudes for the same lengths.

A histogram of the measurement data is shown in Fig. 6 (a) together with the probability density functions (PDFs) for some possible distributions. These are a Rayleigh distribution, a Beta distribution and a log-normal distribution, respectively.

Since the crosstalk channel may be described by a multipath propagation of interfering waves, a Rayleigh distribution seems to be a natural choice to describe the FEXT magnitudes. But the figures show that a Rayleigh distribution does not fit the measurements very well. The measurements have a higher percentage of small amplitudes than presumed by the Rayleigh distribution. This can better be resembled by the Beta distribution for shorter cables, and for longer cables (400m and 600m) the log-normal distribution seems to be more suitable.

2) Second order statistics: A further analysis takes into account second order statistical parameters, i.e., the autocorrelation of the FEXT magnitudes. Fig. 7 (a) shows the normalized autocorrelation functions (ACF) $R_{\tilde{H}\tilde{H}}(k\Delta f)$ of the intra-binder FEXT for the 200m measurements. These ACF are derived from the amplitude of the FEXT transfer functions referenced to the worst case

$$\tilde{H}_{Fext}(f) = \frac{H_{Fext}(f)}{H_{Fext,WC}(f)} \tag{10}$$

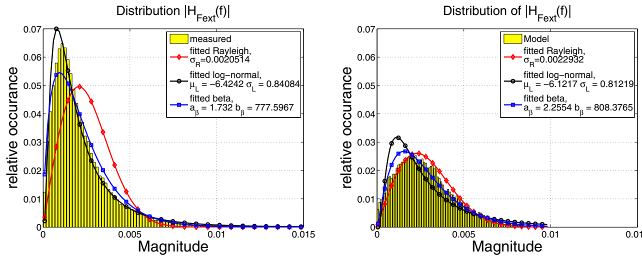

(a) Measurement (b) Model

Fig. 6. Distribution of FEXT magnitudes from measurement and model, 200m cable.

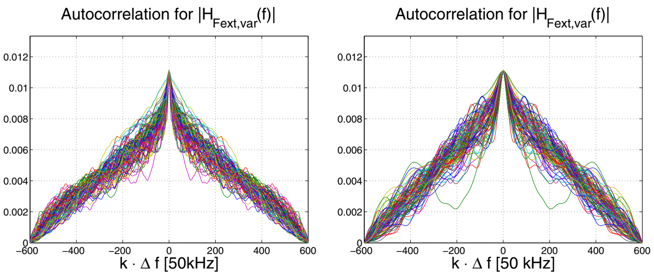

(a) Measurement (b) Model

Fig. 7. Normalized ACF for amplitude of random part of measured and modelled pair-to-pair FEXT, 200m cable.

Then the ACF is given by the expectation value

$$R_{\tilde{H}\tilde{H}}(k \cdot \Delta f) = E\{\tilde{H}_{Fext}(f) \cdot \tilde{H}_{Fext}(f + k \cdot \Delta f)\} \quad (11)$$

B. Statistics of Model Data

The same statistical analysis is carried out for the modelling results.

1) First order statistics: As mentioned before, the FEXT transfer functions generated by the model were scaled by approximately 5 dB to obtain the mean magnitude values comparable to the measurement data, which are shown in Fig. 5 (in logarithmic scale). It can be seen that the mean values as well as the standard deviations fit well to the measurements. Looking at the histogram of the FEXT magnitude distribution in Fig. 6 (b), a difference between measurement and model is still visible. For cable lengths below 300m, the Rayleigh distribution fits better to the model data.

2) Second order statistics: Similarly, the ACF for some example model outputs are shown in Fig 7 (b). It can be seen by comparing the ACF from the measurement to those of the modelling that the curves have a very similar shape. This also indicates similar statistical properties of the model output and the real cable measurement.

V. Conclusions

FEXT is caused by electromagnetic coupling among copper lines. An accurate mathematical description of the FEXT has been a challenging task for a long time. In this study, we propose a MIMO model based on the sum-of-sinusoids method to accurately characterize the DSL FEXT. The model is relatively simple and shows good compliance with our measurement data. First and second order statistical characteristics of the model output and measurement data have been found to be similar. This gives a good reason for applying the presented FEXT model in practice. In fact, this model has successfully been employed in our FEXT relevant simulations, such as in developing and testing FEXT cancellation algorithms.

Future work includes investigations on the applicability of the proposed model (say, with more sinusoid terms) to more commercially available DSL cables, an extension to incorporate the cable geometry (thickness, construction, distances among interfering wires, ...), etc. As NEXT is caused in a similar way as FEXT (see e.g. [10]), the proposed sum-of-sinusoids approach can therefore be employed for modelling NEXT as well.

VI. Acknowledgments

The first two authors would like to thank their colleagues of the Wireline Communications division, Infineon Technologies AG, for their supports and fruitful discussions.

References

[1] P. Silverman, “Draft dynamic spectrum management technical report for second default ballot,” ATIS NIPP-NAI, Tech. Rep., 2007, NIPP-NAI-2007-038R2.

[2] E. Karipidis, N. Sidiropoulos, A. Leshem, L. Youming, R. Tarafi, and M. Ouzzif, “Crosstalk models for short VDSL2 lines from measured 30 MHz data,” *EURASIP Journal on Applied Signal Processing*, pp. 1–9, 2006.

[3] ATIS, *T1.417-2003: Spectrum Management for Loop Transmission Systems*, 2003, American National Standard.

[4] Conexant Systems Inc., *Proposal for Construction of a MIMO Channel Model for Evaluation of FEXT Cancellation Systems*, 2006, Contribution to ATIS NIPP-NAI, NIPP-NAI-2006-169.

[5] J. Verlinden, J. Maes, M. Peeters, and M. Guenach, *Crosstalk Channel Modelling: Detailed Analysis*, 2007, Contribution to ATIS NIPP-NAI, NIPP-NAI-2007-140, Alcatel-Lucent.

[6] J. Verlinden and A. Wilson, *Crosstalk Channel Modelling: Detailed Analysis and Proposal*, 2007, Contribution to ATIS NIPP-NAI, NIPP-NAI-2007-157, Alcatel-Lucent and Adtran.

[7] J. Verlinden, *Crosstalk Channel Modelling: Proposal*, 2007, Contribution to ATIS NIPP-NAI, NIPP-NAI-2007-141, Alcatel-Lucent.

[8] J. M. Cioffi, J. L. Fang, and G. Ginis, “MIMO model for copper cable: Quantitative analysis of matching to measured data,” *IEEE 802.3 Ethernet in the First Mile Task Force*, 03 2002, available at http://grouper.ieee.org/groups/802/3/efm/public/mar02/fang_1_0302.pdf.

[9] J. M. Cioffi, “A temporary model for EFM/MIMO cable characterization,” *IEEE 802.3 Ethernet in the First Mile Task Force*, 09 2001, avalable at http://grouper.ieee.org/groups/802/3/efm/public/sep01/cioffi_1_0901.pdf.

[10] B. Lee, J. M. Cioffi, S. Jagannathan, K. Seong, Y. Kim, M. Mohseni, and M. H. Brady, “Binder MIMO channels,” *IEEE Trans. Commun.*, vol. 55, pp. 1617–1627, 2007.

[11] W. C. Jakes, *Microwave Mobile Communications (Ed.)*. John Wiley & Sons, 1974.

[12] P. A. Hoeher, “A statistical discrete-time model for the WSSUS multipath channel,” *IEEE Trans. Veh. Technol.*, vol. 41, pp. 461–468, 1992.

[13] C. Wang, D. Yuan, H.-H. Chen, and W. Xu, “An improved deterministic SoS channel simulator for efficient simulation of multiple uncorrelated Rayleigh fading channels,” *IEEE Trans. Wireless Commun.*, vol. 7, pp. 3307–3311, 2008.

[14] C. Schroeder, “MIMO channel modelling for DSL crosstalk cancellation,” Master’s thesis, University of Kiel, Information and Coding Theory Lab, 2008.

[15] J. Verlinden, *Crosstalk Channel Model: Text Proposal*, 2008, Contribution to ATIS NIPP-NAI, NIPP-NAI-2008-010R1, Alcatel-Lucent.